Tight Binding of Deoxyribonucleotide Triphosphates to Human Thymidine Kinase 2 Expressed in *Escherichia coli*. Purification and Partial Characterization of Its Dimeric and Tetrameric Forms†

João Filipe Barroso, Morten Elholm,‡ and Torgeir Flatmark*

Department of Biochemistry and Molecular Biology, University of Bergen, Jonas Lies vei 91, N-5009 Bergen, Norway

Received July 11, 2003; Revised Manuscript Received September 12, 2003

ABSTRACT: Human thymidine kinase 2 (hTK2) phosphorylates pyrimidine deoxyribonucleosides to the corresponding nucleoside monophosphates, using a nucleotide triphosphate as a phosphate donor. In this study, hTK2 was cloned and expressed at high levels in *Escherichia coli* as a fusion protein with maltose-binding protein. Induction of a heat-shock response by ethanol and coexpression of plasmid-encoded GroEL/ES chaperonins at 28 °C minimized the nonspecific aggregation of the hybrid protein and improved the recovery of three homooligomeric forms of the properly folded enzyme, i.e., dimer > tetramer > hexamer. The dimer and the tetramer were isolated in stable and highly purified forms after proteolytic removal of the fusion partner. Both oligomers contained a substoichiometric amount of deoxyribonucleotide triphosphates (dTTP > dCTP > dATP), known to be strong feedback inhibitors of the enzyme. Steady-state kinetic studies were consistent with the presence of endogenous inhibitors, and both oligomeric forms revealed a lag phase of at least ∼5 min, which was abolished on preincubation with substrate (dThd or dCyd). The rather similar kinetic properties of the two oligomeric forms indicate that the basic functional unit is a dimer. Molecular docking experiments with a modeled hTK2 three-dimensional structure accurately predicted the binding positions at the active site of the natural substrates (dThd, dCyd, and ATP) and inhibitors (dTTP and dCTP), with highly conserved orientations obtained for all ligands. The calculated relative nonbonded interaction energies are in agreement with the biochemical data and show that the inhibitor complexes have lower stabilization energies (higher affinity) than the substrates.

Four distinct human deoxyribonucleoside kinases are responsible for initiating the salvage of deoxyribonucleosides by catalyzing their irreversible phosphorylation to monophosphates, which can be further phosphorylated to triphosphates by nucleoside mono- and diphosphate kinases (reviewed in ref *1*). Thymidine kinase 1 (TK1)[1] has the most restricted substrate specificity since it only phosphorylates 2′-deoxythymidine (dThd) and 2′-deoxyuridine (dUrd). Deoxycytidine kinase (dCK) phosphorylates 2′-deoxycytidine (dCyd), 2′-deoxyadenosine (dAdo), and 2′-deoxyguanosine (dGuo). Deoxyguanosine kinase (dGK) can efficiently phosphorylate dGuo, dAdo, and 2′-deoxyinosine (dIno). Thymidine kinase 2 [2′-deoxythymidine kinase (TK2, EC 2.7.1.21)] phosphorylates dThd, dCyd, and dUrd. TK1 and dCK have been shown to be cytosolic enzymes, although dCK may enter the nucleus under certain conditions (*2*). By contrast, dGK and TK2 are predominantly mitochondrial enzymes (*3*−*6*), but TK2 may also be present in the cytosol (*3*, *7*−*10*). Furthermore, the expression of TK1 is strictly correlated to the S phase in contrast to the other three enzymes, which are constitutively expressed. This makes TK2 the only thymidine phosphorylating enzyme expressed in nonproliferating tissues, and together with dGK and dCK, it is important in providing precursors for DNA repair and/or mitochondrial DNA (mtDNA) replication in resting cells, lacking *de novo* synthesis (reviewed in ref *1*). TK2 and dGK together phosphorylate all naturally occurring deoxyribonucleosides and may be sufficient or even essential in resting cells by providing the necessary dNTPs for mtDNA replication. Thus, their vital role in maintaining balanced mitochondrial dNTP pools has been proven by the discovery of mutations in the genes of both enzymes associated with inherited and severe mtDNA depletion syndromes (*11*−*13*).

The human deoxyribonucleoside kinases are preferentially feedback regulated by the end product deoxyribonucleotide triphosphates of their preferred substrates, representing a fine regulatory mechanism in the maintenance of a balanced pool

† This work was supported by the Fundação para a Ciência e a Tecnologia (FCT), Portugal, Grant PRAXIS XXI/BD/21690/99, and the Research Council of Norway (NFR).

* To whom correspondence should be addressed. Telephone: (47) 55 58 64 28. Fax: (47) 55 58 63 60. E-mail: torgeir.flatmark@ibmb.uib.no.

‡ Present address: Division of Nutritional Sciences, Cornell University, Ithaca, NY 14853.

[1] Abbreviations: TK2, thymidine kinase 2; hTK2, human TK2; TK1, thymidine kinase 1; dCK, deoxycytidine kinase; dGK, deoxyguanosine kinase; *Dm*-dNK, *Drosophila melanogaster* deoxynucleoside kinase; TK_{HSV1}, herpes simplex virus type 1 thymidine kinase; dThd, 2′-deoxythymidine; dCyd, 2′-deoxycytidine; dTMP, 2′-deoxythymidine monophosphate; dCMP, 2′-deoxycytidine monophosphate; dNTP, deoxyribonucleotide triphosphate; dTTP, 2′-deoxythymidine triphosphate; dCTP, 2′-deoxycytidine triphosphate; dATP, 2′-deoxyadenosine triphosphate; mtDNA, mitochondrial DNA; hsps, heat-shock proteins; MBP, maltose-binding protein; IPTG, isopropyl thio-β-D-galactoside; BSA, bovine serum albumin; GFP, green fluorescence protein; HPLC, high-performance liquid chromatography; t_R, retention time; *h*, Hill coefficient; $[S]_{0.5}$, substrate concentration yielding half-maximum saturation.

10.1021/bi035230f CCC: $25.00
Published on Web 12/03/2003

of dNTPs since these kinases usually catalyze the rate-limiting step in the salvage pathway. Experimental evidence has been presented (*14*, *15*) that dNTPs may form tight inhibitory complexes with the enzyme's active site, acting as bisubstrate analogues, with the deoxyribonucleoside moiety binding, with high specificity, to the deoxyribonucleoside binding site on the enzyme and the triphosphate group fitting into the phosphate donor subsite. This model has just recently been proven for the *Drosophila melanogaster* deoxynucleoside kinase (*Dm*-dNK), with the crystallization of the enzyme in complex with its feedback inhibitor MgdTTP (*16*), and seems to be applicable to the human enzymes given that such a binding position was obtained for ATP in the crystal structure of human dGK (*17*).

In the paper presented here, we report on the cloning of the hTK2 cDNA and its high-level expression in *Escherichia coli* as a soluble fusion protein with maltose-binding protein (MBP), and the purification and functional characterization of two active oligomeric forms. Co-overexpression of plasmid-encoded GroEL/ES chaperonins and simultaneous ethanol supplementation of the growth medium, which induces a heat-shock response in the bacteria, were found to be essential to improve the recovery of the soluble oligomeric forms. We also present evidence that recombinant hTK2, as isolated from *E. coli*, contains different deoxyribonucleotide triphosphates, known to be potent feedback inhibitors of the enzyme. A molecular docking study of substrates and deoxyribonucleotide triphosphates docked into a modeled hTK2 three-dimensional (3D) structure, created by using *Dm*-dNK as a template, was performed to further analyze their binding modes and relative binding affinities. Finally, the subcellular localization of the enzyme, notably, the possibility of a cytosolic localization in addition to the generally considered mitochondrial one, is discussed.

EXPERIMENTAL PROCEDURES

Cloning of hTK2 cDNA. hTK2 specific primers (MWG-Biotech AG) (3-5′-caagtt**atg**ggtgcgttctgccagcg-3′-28 forward primer and 725-5′-acctttgcctc**cta**tgggcaatgc-3′-701 reverse primer, with initiation and stop codons in bold type; coordinates from GenBank entry U77088) were used in a RT-PCR to clone the entire coding region of the hTK2 cDNA (GenBank entry U77088) using total RNA extracted with TRIZOL (Gibco BRL) from Hep2 cells grown to 66% confluence. The cDNA was synthesized using the GeneAmp RNA PCR kit (Perkin-Elmer Life and Analytical Sciences) according to the protocol. The amplified PCR product was cloned into the pCR 2.1-TOPO vector (Invitrogen) and transformed into TOP10 cells. *Bam*HI and *Sal*I restriction sites were introduced into the hTK2 cDNA by PCR (5′-gtcaggatcc-9-**atg**ggtgcgttctgccagcg-3′-28 forward primer and 5′-gtcagtcgac-725-acctttgcctc**cta**tgggc-3′-706 reverse primer, with initiation and stop codons in bold type). The obtained product was cloned into the pMal-c2 vector (New England Biolabs) and transformed into BL21*trxB*(DE3) cells (Novagen), either alone or together with the pGroESL plasmid (obtained from A. A. Gatenby, E. I. DuPont de Nemours & Co.), which encodes the *groE* operon under the control of both the native and the *lac* promoter. The sequence was confirmed by sequencing of both DNA strands using the BigDye Terminator Cycle Sequencing Kit on an ABI PRISM 377 DNA sequencer (Applied Biosystems).

Expression and Purification of Recombinant hTK2. The pMAL expression system was used for the overproduction of the MBP−$(pepIEGR)_{Xa}$−hTK2 fusion protein, with maltose-binding protein (MBP) as the stabilizing fusion partner. Cells were grown at 37 °C, and expression of hTK2 was induced at 28 °C by the addition of 1 mM isopropyl thio-β-D-galactoside (IPTG), when the OD_{600} equaled ~0.8. All media contained 200 μg/mL ampicillin and 30 μg/mL kanamycin, with 60 μg/mL chloramphenicol when co-overexpressing GroEL/ES. Ethanol was added to the medium prior to inoculation at a final concentration of 3% (v/v) when indicated. The cells were harvested 4 or 24 h after induction, and the pellets were kept at −20 °C until they were used. The bacteria were resuspended in a medium containing 10 mM Tris-HCl, 0.2 M NaCl, 2 mM DTT, 10 mM benzamidine, 1 mM EDTA, 2 μg/mL leupeptine, 0.5 μg/mL pepstatine, and 1 mM PMSF (pH 7.25) and disrupted by being passed through a French press (type FA-073 from SLM Instruments, Urbana, IL). After protein purification by affinity chromatography on amylose resin (New England Biolabs) (*18*) and size-exclusion chromatography (see below) at 4 °C, the isolated fusion proteins were cleaved overnight (approximately 16 h) at 4 °C by the restriction protease factor Xa (Protein Engineering Technology ApS) using a protease to hTK2 ratio of 1:150 (w/w) and applied to a second column of amylose resin, to remove MBP. The tetrameric and dimeric forms were isolated by size-exclusion chromatography at 4 °C using a HiLoad Superdex 200 HR column (1.6 cm × 60 cm) prepacked from Amersham Biosciences, and aliquots were stored in liquid nitrogen until they were used. The relative molecular mass of the protomer and the purity of the isolated recombinant protein were analyzed by 15% SDS−PAGE. The protein concentration was determined by the Bradford protein assay (Bio-Rad), using BSA as the standard.

Oligomeric Forms of hTK2. The relative molecular mass of the different oligomeric forms of hTK2 was determined by analytical size-exclusion high-performance liquid chromatography (HPLC) using a TSK-GEL $G3000SW_{XL}$ column (Tosoh Bioscience), at room temperature. The relative molecular mass of the different oligomeric forms was estimated from a calibration curve obtained with the following standard proteins: cytochrome *c* (12.4 kDa), myoglobin (17.8 and 35.6 kDa), soybean trypsin inhibitor (20.1 kDa), chymotrypsinogen A (25 kDa), ovalbumin (43, 86, and 129 kDa), BSA (68, 136, and 204 kDa), human transferrin (74, 148, and 222 kDa), MBP−phenylalanine hydroxylase (186 and 372 kDa), and thyroglobulin (669 kDa). Blue dextran and dTMP were used to determine the void volume (V_0 = 6.24 mL) and the total exclusion volume (V_T = 12.22 mL) of the column, respectively.

Chromatographic Analysis of Bound Deoxyribonucleotides. The deoxyribonucleotides bound to hTK2 were released from the protein by 4% (w/v) perchloric acid precipitation and identified and/or quantified by anion-exchange HPLC analysis using a PartiSphere-5 SAX column (prepacked by Whatman) coupled to a Shimadzu HPLC LC-10Avp system with an SPD-M10Avp UV−vis photodiode array detector (Shimadzu). Data acquisition and processing were performed with the CLASS VP software (Shimadzu).

Assay of hTK2 Activity. The assay of hTK2 activity was based on the quantitative separation of radiolabeled nucleo-

sides and nucleotides by HPLC (*19*). The activity was measured at 25 °C in a 50 μL standard reaction mixture containing 50 mM Na-Hepes (pH 7.5, 25 °C), 5 mM DTT, 0.05% (w/v) BSA, 600 μM $MgCl_2$, 300 μM ATP, 200 μM tritium-labeled substrate, and 1 μg/mL recombinant hTK2, unless otherwise indicated. The enzyme was preincubated at 25 °C for 5 min with the substrate (dThd or dCyd) before the reaction was initiated by the addition of MgATP. The reaction was then allowed to proceed for 5 min and was stopped by adding 1 volume of ice-cold 2% (v/v) acetic acid in ethanol (pH 4.0). For each different substrate concentration used in the assays, duplicates of the reaction were made, with an average variance of $<5\%$, and a correction blank was made by performing the reactions in the absence of enzyme. The phosphorylated product dTMP or dCMP was isolated by HPLC on a PartiSphere-5 SAX column, and the radioactivity was determined by scintillation counting. The recovery of HPLC-grade standard nucleotides from this column was $\geq 95\%$. The steady-state enzyme kinetic parameters were calculated by nonlinear regression analysis using the SigmaPlot Technical Graphing Software (SPSS Inc.) and the Hill equation. In some experiments, the time course of the reaction was followed in a standard reaction incubation mixture containing 5 μg/mL hTK2, to study the effect of substrate preincubation on the specific activity of the enzyme. Three different experimental conditions were studied: (i) dThd or dCyd preincubation for 5 min before the reaction was started with MgATP, (ii) MgATP preincubation for 5 min before the reaction was started with dThd or dCyd, and (iii) no preincubation and the reaction started by adding both substrates at the same time.

Intrinsic Tryptophan Fluorescence Measurements. The intrinsic tryptophan fluorescence of hTK2 was measured on a Perkin-Elmer LS-50B instrument at 25 °C in a buffer containing 20 mM Na-Hepes and 0.2 M NaCl (pH 7.0) and a protein concentration of 0.03 mg/mL. The excitation and emission wavelengths were 295 and 338 nm, respectively. To study the effect of the substrates, increasing concentrations of dThd (from 0.5 to 2000 μM) or MgATP (from 5 to 1500 μM; 2:1 $MgCl_2$:ATP ratio) were added to the incubation mixture every time equilibrium was achieved after the previous addition, and the change in fluorescence intensity (ΔF_{338}) was measured as a function of the concentration of added dThd or MgATP. Nonlinear regression analysis of the data (the binding isotherm) was performed as described above.

Modeling of hTK2 and Molecular Docking of Substrates and Inhibitors. A modeled 3D structure of hTK2 was prepared by comparative protein modeling using the SWISS-MODEL computer algorithm (*20*−*22*) and *Dm*-dNK as the template (PDB entry 1J90) (*17*). The DOCK 4.0.1 suite of programs (University of California, San Francisco, CA) (*23*, *24*) was used to fit different ligands into the active site of the modeled hTK2 structure. The solvent-accessible surface of the structure was calculated by the DMS program under MidasPlus (University of California) (*25*). The active site was identified and filled with sphere centers describing the shape of the molecular surface (*26*), and scoring grids were generated (*27*, *28*). During the docking procedure, spheres are matched with ligand atoms and the scoring grids used to evaluate possible ligand orientations by analyzing the steric boundary of the protein and electrostatic and van der Waals interactions between the protein and the ligand atoms (contact and force field scoring scheme), yielding an intermolecular interaction energy. The atom potentials and the partial charges of the ligands were assigned for the AMBER force field using InsightII (Accelrys). A grid space of 0.2 Å, a dielectric factor of 4, and a sampling size of 5000 structures were used. The DOCK program does not allow for flexibility of the protein during the docking procedure, but optimization of the bound ligand structure was accomplished during docking by allowing the flexibility of the ligands. Final optimization of the structure of the complexes that were obtained was performed by energy minimization using Discover (Accelrys). The programs InsightII and DS ViewerPro (Accelrys) were used to prepare the figures of the docked conformers.

RESULTS

Cloning of Recombinant hTK2. With the use of specific primers, the hTK2 cDNA published by Johansson *et al*. (*8*) was cloned from Hep2 cells. The hTK2 primary sequence presented here differs from the one reported by Johansson *et al*. in two amino acids. At position 30 we found a Ser instead of a Gly and at position 143 an Ala instead of a Val. The cDNAs published by Wang *et al*. (*6*, *29*) also encode a Ser at position 30, but codon 143 encodes a Val residue.[2] From the published human genome sequence (*30*), it is possible to predict a Ser and a Val at positions 30 and 143, respectively, from the hTK2 gene (GenBank entry AC010289). The residue at position 30 is part of the P-loop, a highly conserved region in deoxyribonucleoside kinases, important for the binding of the triphosphate group of the phosphate donor nucleotide. Although this residue is not conserved among the different mammalian kinases, a Ser residue is always present in a group of TK2-like enzymes (*31*). Amino acid 143 does not appear to occupy any region critical for catalysis or oligomerization, nor is it conserved in the deoxyribonucleoside kinase family. Furthermore, exchange between a Val and an Ala, when buried, belongs to so-called "safe" residue substitutions (*32*), which are unlikely to affect the protein structure. In the hTK2 modeled structure (see below), the side chain from amino acid 143 is facing a hydrophobic microenvironment formed by residues Leu87, His90, Ile105, His106, Ile137, Leu138, Met141, and Val145, all within 8 Å.

Effect of GroEL/ES Overexpression and Ethanol Supplementation on the Recovery of the Soluble Fusion Protein. The MBP−hTK2 fusion protein aggregated extensively when overexpressed for 4 h in *E. coli* at 28 °C (Figure 1A), providing a very low recovery of the soluble protein. Only a small improvement in the solubility was obtained by co-overexpressing the GroEL/ES molecular chaperone system (Figure 1C), whereas ethanol supplementation, which induces a heat-shock response in the bacteria (*33*−*35*), made a remarkable positive contribution to the recovery of soluble compared to aggregated protein (Figure 1B). Furthermore, a small synergistic effect was observed by the combined use

[2] The numbering used here is based on the hTK2 sequence published by Johansson *et al*. (*8*). Different numbering is found in the two hTK2 sequences published by Wang *et al*., i.e., Ser28 and Val141 (*29*) or Ser61 and Val174 (*6*), because of differences in the N-terminal part of the protein.

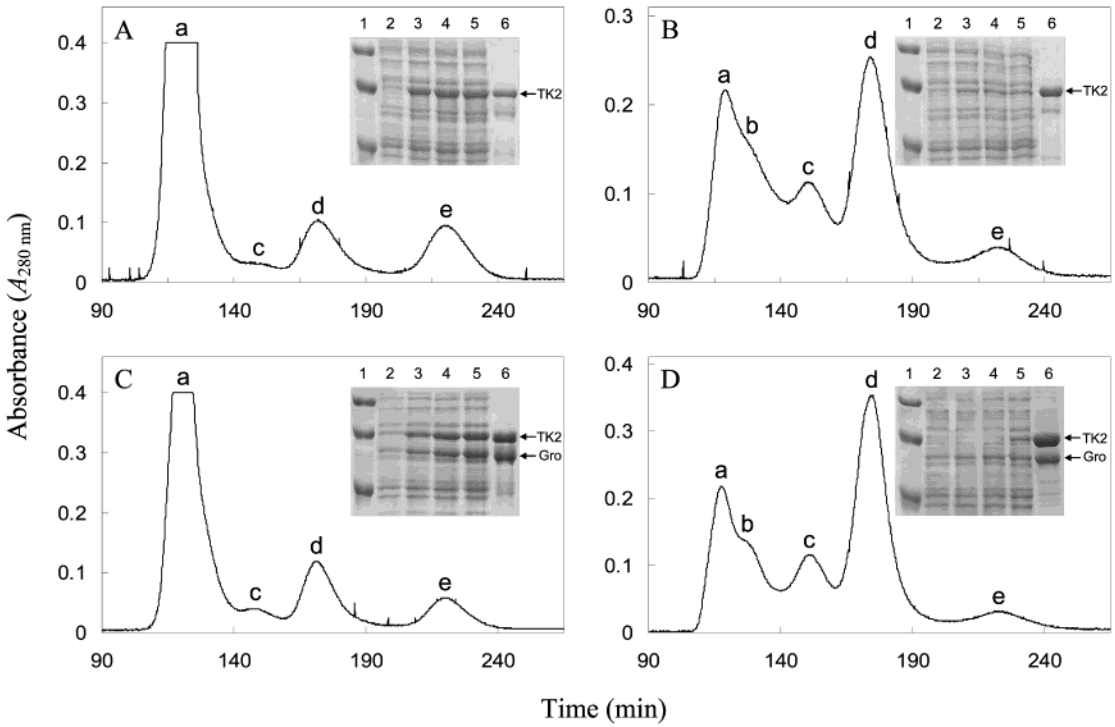

FIGURE 1: Size-exclusion chromatography on the Superdex 200 column of the recombinant MBP−hTK2 fusion proteins obtained after induction for 4 h at 28 °C with different growth and expression conditions: (A) without GroEL/ES co-overexpression or ethanol supplementation, (B) with ethanol supplementation, (C) with GroEL/ES co-overexpression, and (D) with ethanol supplementation and GroEL/ES co-overexpression. Peak a, high-molecular mass aggregates and higher oligomeric forms; peak b, hexamer (∼420 kDa); peak c, tetramer (∼280 kDa); peak d, dimer (∼140 kDa); and peak e, degradation products (∼40 kDa). The column was equilibrated in 20 mM Na-Hepes and 0.2 M NaCl (pH 7.0, 23 mL/h). Ten milligrams of fusion protein was loaded on the column in each experiment. The insets represent 10% SDS−PAGE monitoring protein expression as a function of the induction time: lane 1, molecular mass markers (97.4, 66.2, and 45.0 kDa); lanes 2−5, total protein content of the bacteria immediately before induction with IPTG and after induction for 1, 2, and 4 h, respectively; and lane 6, protein recovered from the amylose resin. The positions of the MBP−hTK2 fusion protein (TK2) and GroEL (Gro) are denoted with arrows.

of ethanol addition and GroEL/ES coexpression (Figure 1D). GroEL was consistently copurified with the fusion protein on the affinity chromatography step, but it was mainly associated with the high-molecular mass aggregates as revealed by SDS−PAGE (Figures 1 and 2). The reduced level of expression of the MBP−hTK2 fusion protein upon ethanol supplementation, as observed by SDS−PAGE (Figure 1), was overcome by a longer induction period (24 h), without any significant change in the relative proportion between the oligomeric forms (data not shown). A total yield of the purified MBP−hTK2 fusion protein ranging from 80 to 100 mg/L of bacterial culture was obtained after induction for 24 h. The nonaggregated MBP−hTK2 fusion protein was recovered as a mixture of dimers, tetramers, and hexamers, with the dimer as the dominant oligomeric form. The hexameric form of the fusion protein was not further studied because of its incomplete separation from the aggregated forms (Figures 1 and 2) and a stronger tendency to aggregate.

Purification of Recombinant hTK2. The fractions of isolated dimeric and tetrameric fusion proteins obtained from size-exclusion chromatography were cleaved overnight (approximately 16 h) with factor Xa (4 °C), which resulted in a near-complete cleavage of the fusion protein (Figure 2) with minimal aggregation and no apparent loss of enzyme activity. Because of the similar relative molecular mass of MBP and isolated dimeric hTK2, the fusion partner and any remaining uncleaved protein were removed by passing the protein over a second column of amylose resin (Figure 2). The different oligomeric forms of hTK2 were further purified

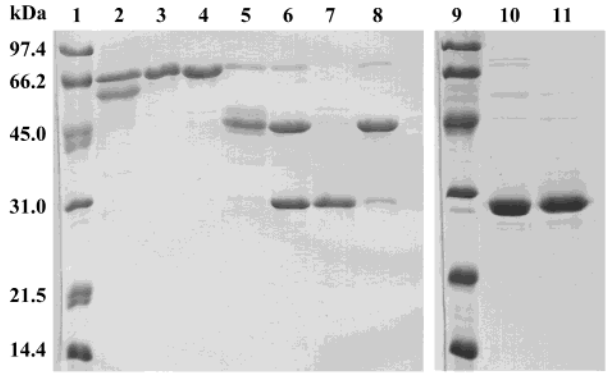

FIGURE 2: SDS−PAGE of the purification of the recombinant hTK2 enzyme expressed for 24 h with GroEL/ES co-overexpression and ethanol supplementation of the growth medium. Lanes 1 and 9 contained molecular mass markers. Lanes 2−5 represent peaks b−e, respectively, from size-exclusion chromatography on the Superdex 200 column (Figure 1B and D). Lane 2 contained high-molecular mass aggregates, hexameric fusion protein, and GroEL. Lane 3 contained the isolated tetrameric fusion protein. Lane 4 contained the isolated dimeric fusion protein. Lane 5 contained degradation products (∼40 kDa). Lane 6 contained the isolated dimeric fusion protein cleaved (incubation for 16 h) with factor Xa, which was sequentially applied to a column of amylose resin. Lane 7 contained pure hTK2, collected as the flow-through from amylose resin and later loaded on a Superdex 200 size-exclusion column. Lane 8 contained isolated MBP and uncleaved fusion protein eluted from the amylose column with maltose. Lane 10 contained isolated tetrameric hTK2, from the Superdex 200 column. Lane 11 contained isolated dimeric hTK2, from the Superdex 200 column.

by a second size-exclusion chromatographic step, yielding homogeneous preparations of tetrameric and dimeric hTK2 with single bands on SDS−PAGE (>97% pure) at a relative molecular mass of ~27.5 kDa (Figure 2). Under optimum conditions, approximately 10 mg of highly pure and soluble hTK2 was obtained per liter of culture.

Oligomeric Forms of hTK2 and Identification of Its Bound Deoxyribonucleotides. The isolated cleaved hTK2 subjected to size-exclusion chromatography on a Superdex 200 column eluted in three peaks with relative molecular masses of ~170100, ~108000, and ~50900 Da, which matched the masses of hexameric, tetrameric, and dimeric forms, respectively, of a globular protein with an expected subunit mass of 27.5 kDa. However, due to the discrepancies between the native molecular mass previously reported for mouse TK2 and *Dm*-dNK when analyzed on Superose 12 (highly cross-linked agarose matrix) or Superdex 200 (cross-linked agarose and dextran matrix) columns (*31*, *36*, *37*), we have confirmed our finding by using a TSK-GEL G3000SW$_{XL}$ analytical size-exclusion HPLC column (silica-based matrix). Isolated tetrameric and dimeric forms of virtually pure hTK2 (>97% pure on SDS−PAGE; see Figure 2) revealed the same oligomeric forms as on Superdex 200, with relative molecular masses of ~152200, ~95900, and ~48800 Da for the hexamer, tetramer, and dimer, respectively (Figure 3). Furthermore, the preparations of dimeric and tetrameric hTK2 isolated by chromatography on Superdex 200 were relatively homogeneous, as determined from the integrated areas of the individual components in the chromatographic profiles (see the legend of Figure 3). Moreover, on analytical size-exclusion chromatography (G3000SW$_{XL}$ column) of tetrameric hTK2 and of an approximately 1:1 mixture of tetrameric and dimeric hTK2, no changes in the tetramer ↔ dimer equilibrium toward any of the two forms were observed in the concentration range of 2.0−0.05 mg/mL (data not shown). To test the possible effect of substrates on the oligomeric state of hTK2, the enzyme was preincubated with 300 μM or 3 mM dThd or MgATP before high-performance size-exclusion liquid chromatography on the TSK-GEL G3000SW$_{XL}$ analytical column. Although no significant changes in the relative integrated areas of the chromatographic peaks of the tetramer and dimer were observed on incubation with either ligand, a nonexpected peak, eluting near the total exclusion volume of the column, appeared (data not shown). To our surprise, isolated hTK2 seemed to have some low-molecular mass compound(s) bound to it, which appeared to be released by preincubation with 300 μM dThd. The presence of deoxyribonucleotides in the enzyme preparations was confirmed by anion-exchange HPLC and UV detection (Figure 4). Three different peaks, with retention times (t_R) and λ_{max} values corresponding to those of dTTP, dCTP, and dATP, were isolated from the low-molecular mass compounds released from hTK2 by perchloric acid precipitation, and their relative occupancies were calculated to be 0.46 mol of dTTP, 0.34 mol of dCTP, and 0.02 mol of dATP per mol of hTK2 protomer for the dimeric enzyme (Figure 4). The two major nucleotides bound to hTK2, i.e., dTTP and dCTP, are known to be the two most powerful natural inhibitors of the enzyme (*3*, *6*, *38*, *39*).

Steady-State Kinetic Analysis of Recombinant hTK2. The steady-state kinetic properties of wild-type recombinant hTK2 expressed in *E. coli* have so far been published for a

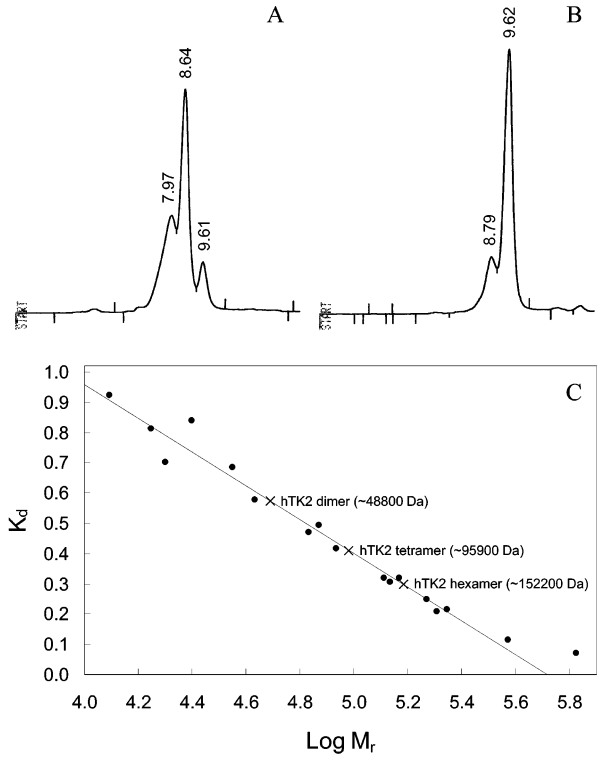

FIGURE 3: Analytical size-exclusion chromatography of isolated recombinant hTK2 on a G3000SW$_{XL}$ HPLC column equilibrated in 20 mM Na-Hepes and 0.2 M NaCl (pH 7.0, 1 mL/min), and molecular mass determination of the different oligomeric forms. (A) Tetrameric hTK2 isolated with Superdex 200. The integrated areas (arbitrary units) are 1 194 900 (t_R = 7.97 min, hexamer), 1 707 100 (t_R = 8.64 min, tetramer), and 366 510 (t_R = 9.61 min, dimer). (B) Dimeric hTK2 isolated with Superdex 200. The integrated areas (arbitrary units) are 539 470 (t_R = 8.79 min, tetramer) and 1 990 200 (t_R = 9.62 min, dimer). (C) Column calibration curve obtained with different standard proteins (for details, see Experimental Procedures). $K_d = (V_E - V_0)/(V_T - V_0)$, where V_E is the elution volume, V_0 is the void volume of the column, and V_T is the total exclusion volume of the column. Twenty micrograms (1 mg/mL) of hTK2 tetramer and dimer, obtained by size-exclusion chromatography on Superdex 200 (as in Figure 1), were loaded on the column in each experiment. Detection was at 280 nm.

dimeric form (*6*, *29*) and a proposed monomeric form (*3*, *39*); however, in no case were there indications of the occurrence of higher oligomeric forms, nor was the possibility considered that the enzymes contained endogenous deoxyribonucleotide inhibitors. In the study presented here, we have compared the kinetic properties of essentially dimeric and tetrameric forms of hTK2 as isolated. First, both oligomeric forms revealed a pronounced (~5 min) lag phase with dThd or dCyd as the substrate, which was completely abolished after preincubation for 5 min with 200 μM dThd (or dCyd), and partially with 300 μM MgATP (Figure 5; data not shown for dCyd). Thus, in the substrate saturation experiments, a 5 min preincubation of the enzyme with the final substrate (dThd or dCyd) concentration was performed before starting the reaction with MgATP. As shown by the results presented in Figure 6 and Table 1, dimeric and tetrameric hTK2 displayed complex kinetic patterns with both dThd and dCyd as the variable substrate. A kinetic cooperativity was observed in Hill plots, which gave two Hill coefficients for both substrates (Figure 6 and Table 1). Thus, a strong negative cooperativity ($h \approx 0.5$) was observed below

Table 1: Steady-State Kinetic Constants of Recombinant Human TK2 As Isolated[a]

	dThd			dCyd			MgATP		
	K_m (μM)	V_{max} (nmol min^{-1} mg^{-1})	h	K_m (μM)	V_{max} (nmol min^{-1} mg^{-1})	h	K_m (μM)	V_{max} (nmol min^{-1} mg^{-1})	h
dimer	54 ± 12	573 ± 41	0.53/0.77	25.1 ± 2.6	277.4 ± 8.7	0.94/0.77	4.7 ± 0.6	481 ± 12	0.83 ± 0.09
tetramer	50 ± 10	537 ± 28	0.49/0.70	18.3 ± 1.8	264.4 ± 6.7	0.86/0.66	10.9 ± 1.7	550 ± 19	0.74 ± 0.08

[a] The values were from two independent assays. The kinetic parameters were calculated by nonlinear regression analysis of the experimental data using the Hill equation. The concentrations of dThd and dCyd were varied from 0.05 to 300 μM, with the ATP concentration kept constant at 300 μM (600 μM $MgCl_2$), and the ATP concentration was varied from 0.5 to 2000 μM (2:1 $MgCl_2$:ATP ratio), with the dThd concentration kept constant at 200 μM. The Hill coefficients (h) for dThd and dCyd were calculated from Hill plots using the V_{max} values obtained from curve fitting, with two different h values being obtained for substrate concentrations below and above 4 μM. The h values for dThd and dCyd, obtained by nonlinear regression analysis, matched the ones calculated using the Hill plots, at substrate concentrations above 4 μM.

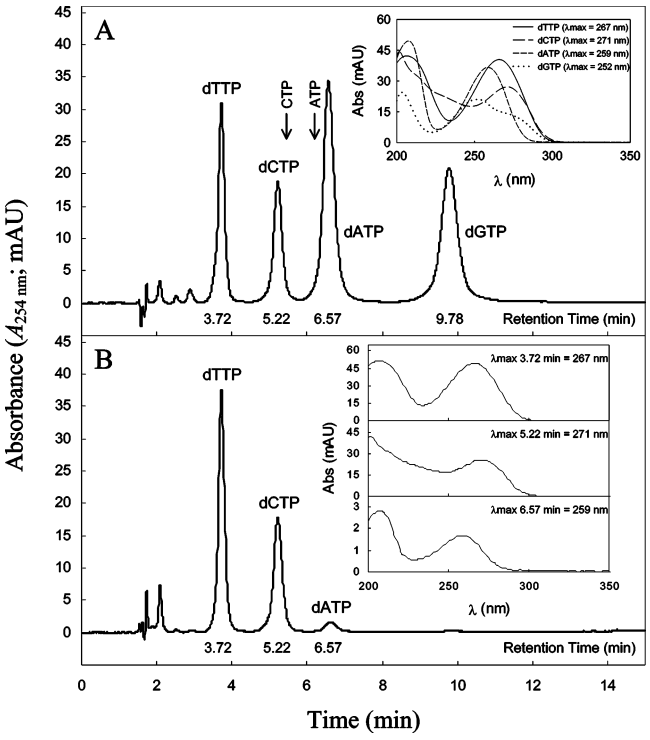

FIGURE 4: Anion-exchange chromatography of deoxyribonucleotides released from isolated hTK2 by perchloric acid precipitation. (A) Chromatogram of a mixture of four deoxyribonucleotide standards (1 nmol of each). (B) Chromatogram of the deoxyribonucleotides released from hTK2 by $HClO_4$ precipitation. The mobile phase was 400 mM KH_2PO_4 and 2% (v/v) *n*-propanol (pH 5.5, 1 mL/min). Retention times (t_R) for each peak are given. The arrows in panel A denote the t_R values for CTP (5.42 min) and ATP (6.20 min). The insets show the absorption spectrum and λ_{max} of each single peak.

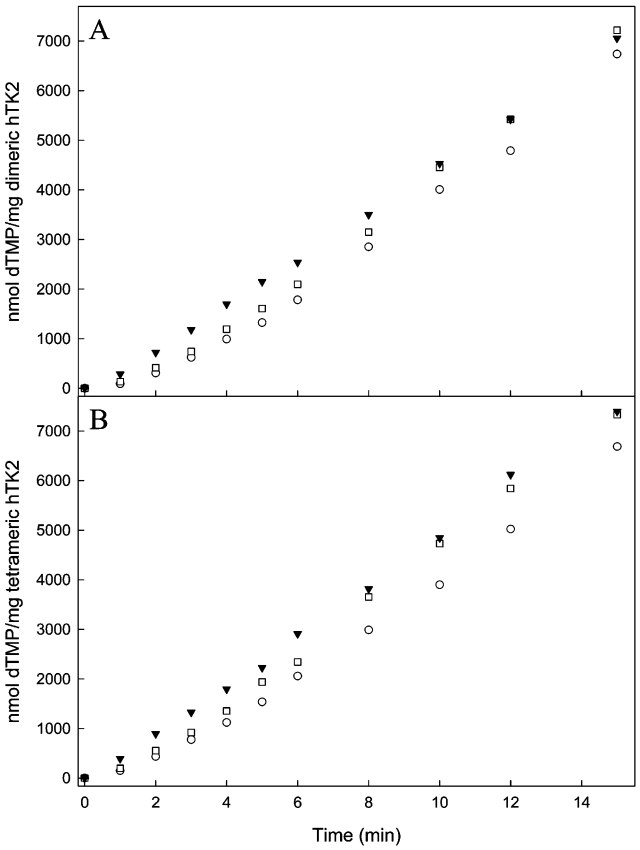

FIGURE 5: Effect of preincubation of recombinant hTK2 with substrate on its catalytic activity. The time course for the hTK2 activity was assayed with 300 μM MgATP and 200 μM dThd for the dimer (A) and tetramer (B), at 25 °C. The different curves correspond to enzyme preincubation (5 min) with no substrate (○), with MgATP (□), or with dThd (▼).

4 μM and a slight negative cooperativity ($h \approx 0.7$) above this concentration, with dThd as the substrate, whereas dCyd followed nearly Michaelis−Menten kinetics at concentrations below 4 μM ($h \approx 0.9$) and gave a slight negative cooperativity ($h \approx 0.7$) above this substrate concentration. The apparent K_m and V_{max} values, obtained by nonlinear regression analysis using the Hill equation, are presented in Table 1. The Hill coefficients obtained by the same method matched the ones calculated using the Hill plots, at substrate concentrations above 4 μM. The kinetic parameters obtained at 25 °C for dimeric hTK2 differ from those previously determined at 37 °C (*6*, *29*). Specifically, the K_m values are ~4 and ~2 times higher for dThd and dCyd, respectively, and the V_{max} values are ~2 and ~3 times lower for dThd and dCyd, respectively. However, the specific activity of our recombinant enzyme showed a 3-fold increase when measured at 37 °C as compared to that measured at 25 °C. With regard to the enzyme's properties toward the phosphate donor MgATP (2:1 $MgCl_2$:ATP ratio), preincubation of the protein with an excess of dThd (200 μM) before the reaction was started resulted in a K_m value for dimeric hTK2 (4.7 μM) 5- and 20-fold lower than the values reported previously for recombinant (*6*) and native enzymes (*38*, *40*), respectively. The tetrameric enzyme revealed a slightly higher K_m value for MgATP (10.9 μM). Hill plots of the experimental data were linear over the concentration range that was tested (0.5−2000 μM), and the Hill coefficients that were obtained were the same as those obtained by nonlinear regression analysis (Table 1).

Intrinsic Tryptophan Fluorescence Measurements. The intrinsic tryptophan fluorescence of the hTK2 dimer showed,

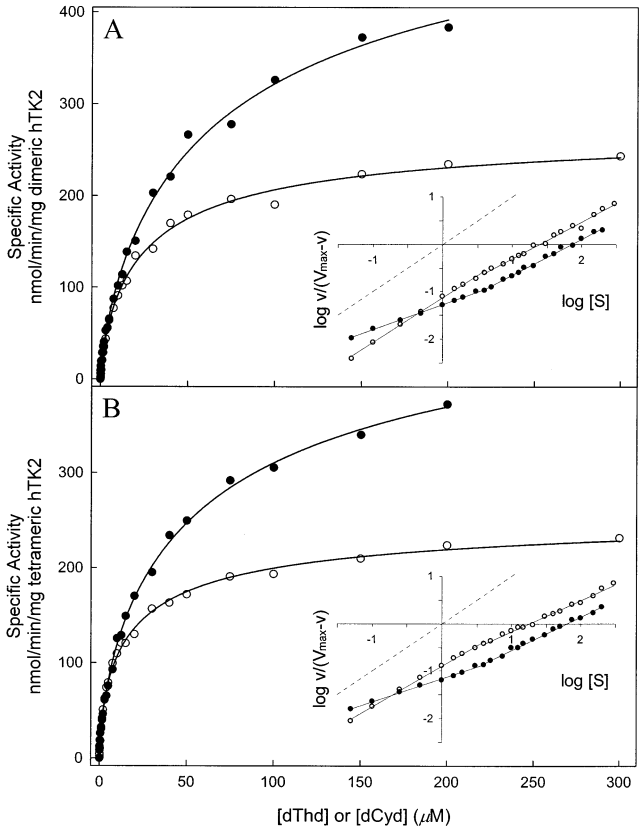

FIGURE 6: Catalytic activity of recombinant hTK2 at varied concentrations of dThd and dCyd. For assay conditions and nonlinear regression analysis, see Experimental Procedures. (A) hTK2 dimer with dThd (●) or dCyd (○) as the variable substrate. (B) hTK2 tetramer with dThd (●) or dCyd (○) as the variable substrate. The fitted curves were obtained using the Hill equation and nonlinear regression analysis. The insets show Hill plots of the same data, with the dashed line indicating a Hill coefficient of 1.0. For all linear regressions, the correlation coefficient (R^2) was equal to or greater than 0.99. The steady-state kinetic constants are summarized in Table 1.

on addition of dThd, a quenching of the fluorescence emission at a λ_{max} of 338 nm. The binding isotherm revealed a biphasic profile (data not shown) with $[S]_{0.5}$ values, calculated by nonlinear regression analysis using the Hill equation, of 4.9 ± 1.3 μM (h = 0.56 ± 0.04) for dThd concentrations below 5 μM and 539.8 ± 16.7 μM (h = 0.92 ± 0.01) for dThd concentrations above 5 μM. A hyperbolic binding isotherm was obtained for the MgATP-induced enhancement of the fluorescence at a λ_{max} of 338 nm (data not shown), with a $[S]_{0.5}$ value of 80.3 ± 6.8 μM (h = 0.94 ± 0.03).

Modeled Structure of hTK2 and Molecular Docking of Substrates and Inhibitors. Despite intensive efforts, no successful crystallization of TK2 has yet been accomplished. However, the high degree of sequence identity between hTK2 and the *Dm*-dNK (40%) (*41*) allowed us to create a 3D structural model of hTK2 by sequence alignment modeling using the SWISS-MODEL computer algorithm (*20*−*22*). Moreover, the substrate-binding site of hTK2 has been described previously for a modeled 3D structure constructed on the basis of *Dm*-dNK (*17*, *42*), and a similar arrangement of the active site residues is observed in our model.

To provide structural and energetic clues related to the substrate specificity of hTK2 and to gain further insight into the proposed binding mode for the end product feedback inhibitors (*14*−*17*), a series of molecular docking experiments were performed on our hTK2 structural model, using the DOCK 4.0.1 suite of programs (*23*, *24*). The pyrimidine natural substrates dThd and dCyd, the phosphate donor ATP, and the feedback inhibitors dTTP and dCTP were all docked into the active site of our modeled hTK2 structure with allowed flexibility of the ligands and optimization of the final bound structure. The 30 top-scoring dock conformers, with respect to shape complementarity (contact score) and molecular mechanics interaction energy (AMBER force field score), obtained for the different ligands were found at very defined positions, with root-mean-square deviation (rmsd) values for all the atoms ranging from 0.29 to 0.82 Å. All configurations of the ligands were located at their expected binding site by analogy with the *Dm*-dNK·dCyd (*17*), *Dm*-dNK·dThd and *Dm*-dNK·dTTP·Mg (*16*), and TK_{HSV1}·ADP·dTMP (*43*) complexes. Figure 7 shows the configurations with the lowest energy scores for the ensemble of 30 conformers obtained for each docked ligand and the residues involved in substrate or inhibitor binding. So far, there are no available structural data for ATP binding at the phosphate donor site of any of the mammalian deoxynucleoside kinases or *Dm*-dNK, although the crystal structure of the herpes simplex virus type 1 thymidine kinase (TK_{HSV1}) in complex with ADP and dTMP (*43*) provides some insight into the phosphate donor binding position. Similarly, in our docked hTK2·ATP complex, phosphate binding occurs mainly within a strand−turn−helix motif termed the P-loop (residues Gly26−Thr33) that accommodates the β-phosphate of ATP and an arginine-rich site called the LID region (residues Arg161−Glu170), and the adenine base is sandwiched with a guanidinium group (Arg161). As expected, both dTTP and dCTP adopted a position characteristic of a bisubstrate analogue, with the nucleoside part bound in the substrate site and the phosphates in the P-loop and LID regions as for the cosubstrate ATP (Figure 7). A few of the 30 scored conformers of dTTP and dCTP show similar phosphate binding as for ATP in the dGK·ATP complex (*17*), but the great majority have the phosphates in a conformation comparable to the one observed in the *Dm*-dNK·dTTP·Mg complex (*16*), with an equivalent hydrogen bonding pattern (Figure 7). The favorable binding of the nucleoside and triphosphate counterparts of the feedback inhibitors in both the substrate and phosphate donor site of the enzyme should give them the capacity to bind their target enzyme with very high specificity and higher affinity than any of the substrates alone. It is thus interesting to note that the feedback inhibitors dTTP and dCTP exhibit lower relative total nonbonded interaction energies (higher affinity) with hTK2 (−75.4 ± 4.7 and − 78.8 ± 6.0 kcal/mol, respectively) than either substrate dThd (−28.0 ± 0.6 kcal/mol) or substrate dCyd (−28.2 ± 0.8 kcal/mol) or cosubstrate ATP (−62.2 ± 0.9 kcal/mol), as judged by the AMBER force field scoring of the DOCK procedure.

DISCUSSION

Cytosolic versus Mitochondrial hTK2. hTK2 has generally been considered to be located in the mitochondria as for the mouse enzyme (*36*, *44*). However, a cytoplasmic localization of the human enzyme has also been suggested (*3*, *7*, *10*). In agreement with such a proposal, a full-length hTK2 cDNA,

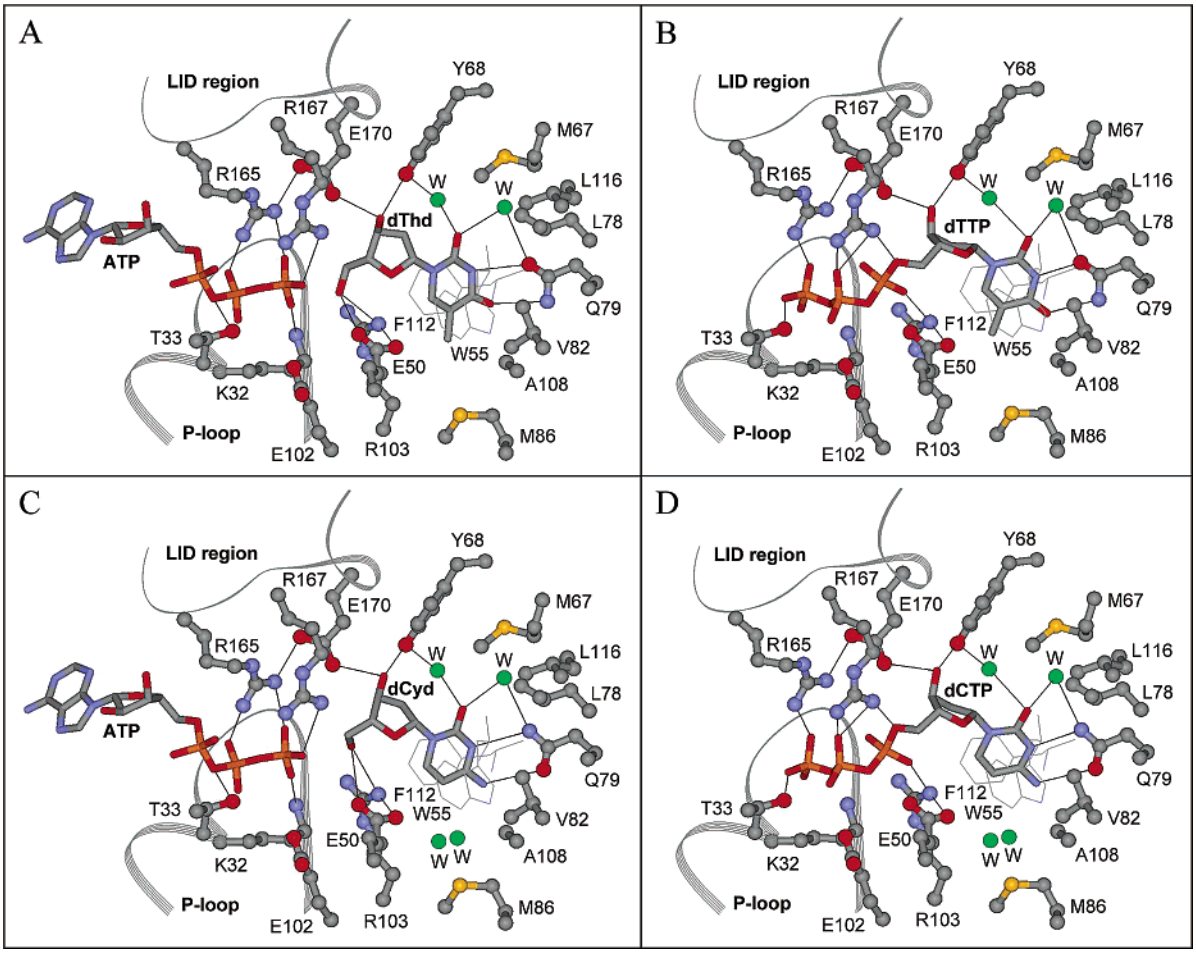

FIGURE 7: Detailed structure of the top-scoring docked conformers of dThd (A), dCyd (C), dTTP (B), dCTP (D), and ATP (A and C) at the active site of the modeled hTK2 structure, obtained with DOCK 4.0.1. Active site residues at the ligand binding sites are shown in ball-and-stick representations, and the different ligands are shown as sticks. For clarity, Trp55 on top of the nucleoside/nucleotide base and Phe112 behind the base are shown as wires. The loops involved in phosphate binding, the P-loop (Gly26−Thr33) and an arginine-rich site called LID (Arg161−Glu170), are shown. Water molecules (W, in green) were taken from the crystal structure of *Dm*-dNK in complex with dCyd (*17*). Hydrogen bonds were calculated with the program InsightII (Accelrys) and are shown as black lines. The β-phosphate of ATP and γ-phosphates of dTTP and dCTP make further interactions with the P-loop main chain (Ala29, Ser30, Lys32, and Thr33), which are not shown for simplicity.

containing an initiation codon and lacking a mitochondrial leader sequence, was cloned (*8*), and the recombinant protein was shown to be predominantly localized to the cytosol on expression in mammalian cells as a GFP fusion protein (*9*). More recently, a full-length recombinant hTK2, containing a mitochondrial targeting signal, was reported, with its 41 N-terminal amino acids differing from the 10 N-terminal residues in the cytosolic isoform but sharing the remaining 224 C-terminal amino acids (*6*). It was suggested that the 5′-sequence of the cDNA lacking a mitochondrial targeting signal is part of an intron sequence, with the coded isoform resulting from an alternatively spliced mRNA product that may not be translated. Nevertheless, by using a specific forward primer directed to this 5′-sequence, we were able to clone the cytosolic isoform again, from Hep2 cells. Thus, it is likely that at least two different forms of the enzyme actually exist in a cell, i.e., a mitochondrial and a cytosolic isoform, as observed for mouse dGK (*45*) and previously suggested for hTK2 (*3*, *7*, *10*). In fact, the hTK2 gene shows multiple transcripts in most tissues (*8*, *29*), and the two isoforms may originate by alternative splicing of alternative first exons, with the hTK2 gene consisting of more exons (for reference, see http://www.ncbi.nlm.nih.gov/IEB/Research/Acembly/av.cgi?db=human&c=Gene&l=TK2) than the 10 initially proposed (*6*). Similar mechanisms have been described previously, notably among proteins involved in DNA metabolism, in which both nuclear/cytosolic and mitochondrial isoproteins originate from a single gene, either by the use of multiple translation initiation sites or by alternative splicing of the gene transcript, which makes the translated proteins identical except for the upstream targeting sequence (*45*−*48*). The coding regions of the first exons from either isoform of hTK2 are closely spaced in the human genome sequence of chromosome 16 (GenBank entry AC010289); the last nucleotide of the first exon in the cytosolic isoform is only 191 bp upstream of the ATG codon from the first exon of the mitochondrial isoform. The mature proteins, i.e., after cleavage of the targeting signal in the mitochondrial isoform, are expected to differ in only the first 8−10 N-terminal amino acids and therefore to have identical catalytic properties. The expression of a cytosolic form of hTK2 will affect the dNTP metabolism and nucleoside analogue activation in ways not considered so far. Thus, compounds phosphorylated by hTK2 may affect not only the mitochondrial but also the nuclear DNA replication and repair, producing a wider range of biological effects.

Effect of GroEL/ES Overexpression and Ethanol Supplementation on the Recovery of the Soluble Fusion Protein. The first attempts to express hTK2 as a MBP fusion protein by standard growth and induction conditions were disappointing since almost no soluble enzyme was obtained due to aggregation, as previously reported for a His tag fusion protein (*49*). However, the problem was solved by co-overexpressing the *E. coli* GroEL/ES chaperon system (*50*−*52*) and simultaneously subjecting the cells to ethanol, which transiently upregulates the synthesis of several heat-shock proteins (hsps) (*33*−*35*, *53*, *54*). While co-overexpression of GroEL/ES alone had little effect on the recovery of the soluble fusion protein, the addition of ethanol prior to inoculation greatly reduced its level of aggregation. Ethanol supplementation before inoculation induces a stoichiometric increase in the intracellular concentration of most chaperones before the induction with IPTG, by stimulating the continuous synthesis of the heat-shock transcription factor σ^{32} (reviewed in ref *55*). Thus, the overexpression of a particular chaperone system is sometimes inadequate since most proteins require the sequential action of several chaperone systems for their correct folding (*56*−*58*). GroEL was copurified with MBP-hTK2 in the affinity chromatography step, and the two proteins formed a stable complex, indicating that the GroEL/ES folding machine (Hsp60/Hsp10 in eukaryotic mitochondria) may exert a direct influence on the folding of hTK2, as occurs for most mitochondrial matrix proteins after import (*59*−*62*). The solubility of hTK2 after expression for 24 h in *E. coli* remained as high as after 4 h. Thus, an important effect of the chaperones may be to prevent the initial formation of small nuclei of aggregated protein and thus avoid the propagation of the self-aggregation of incompletely folded protein. Moreover, in the ethanol-treated cultures, the decreased rate of synthesis of the fusion protein (Figure 1) may also contribute to the high recovery of correctly folded hTK2, by reducing the concentration of aggregation-prone folding intermediates.

Oligomeric Forms of Catalytically Active hTK2. The molecular chaperone-assisted self-assembly of homooligomeric forms of the MBP−hTK2 fusion protein resulted in a mixture of dimers, tetramers, and a minor hexameric form. The dimerization mode of deoxyribonucleoside kinases has been described in the 3D crystal structures of TK_{HSV1} (*63*) and *Dm*-dNK and human dGK (*17*). In our study on hTK2, the dimer constitutes the dominant oligomeric form, representing ∼70% of the soluble protein at pH 7.0 and 4−25 °C. However, to our knowledge, this is the first time higher oligomeric forms (i.e., tetramer and hexamer) have been observed in the class I deoxyribonucleoside kinases, with *Dm*-dNK as the prototype (*64*). Indeed, in a recent report, hTK2 was shown to behave as a dimeric protein on a Superdex 200 size-exclusion chromatography column, with no indications of higher oligomeric forms (*6*). However, in that study (*6*), hTK2 was expressed as a N-terminal His tag fusion protein, which had previously revealed a pronounced tendency to form large aggregates during expression (*49*). The hexameric and tetrameric forms of hTK2 were unequivocally observed in the study presented here when expressed in the presence of an increased level of molecular chaperones (Figure 1). No changes in the oligomeric state were observed in the presence of either dThd or MgATP, confirming the results obtained with native hTK2 isolated from leukemic spleen (*39*).

Isolated hTK2 Is Endogenously Inhibited by Its Natural Feedback Inhibitors. Recombinant hTK2 was recovered from *E. coli* with tightly bound deoxyribonucleotides, i.e., dTTP (0.46 mol/mol of subunit), dCTP (0.34 mol/mol of subunit), and dATP (0.02 mol/mol of subunit). These nucleotides were retained with a high occupancy (∼80%) during the sequential purification steps, indicating that dTTP and dCTP have a very high affinity for hTK2. Such tight binding appears to result from both the highly favorable interactions between the nucleoside moiety and the substrate-binding site and the electrostatic forces provided by the triphosphate group, in the orientation obtained by molecular docking (Figure 7) and recently published for the *Dm*-dNK·dTTP·Mg complex (*16*). Thus, in the inhibitor complexes, the overlap of binding forces characteristic of each set of substrates (e.g., dThd and MgATP) results in a higher affinity of the enzyme for the inhibitors than for either substrate alone, as demonstrated by the force field scoring function of DOCK.

The high dNTP occupancy of recombinant hTK2 repeatedly found in our enzyme preparations suggests that other structurally and functionally related recombinant proteins, produced in *E. coli*, will have at least some inhibitory deoxyribonucleotide triphosphates bound, as isolated. Moreover, native proteins purified from mammalian sources may also be partially inhibited since the average physiological concentrations of dNTPs in mammalian cells, i.e., dTTP (37 ± 30 μM), dCTP (29 ± 19 μM), dATP (24 ± 22 μM), and dGTP (5.2 ± 4.5 μM), are in the same range as the ones found in *E. coli* (dTTP measured up to 100 μM) (*65*).

Steady-State Kinetic Analysis of Endogenously Inhibited Recombinant hTK2. From an enzyme kinetic point of view, we are dealing with a recombinant form of hTK2, which occurs as both a homotetramer and a homodimer in some sort of equilibrium. Moreover, both enzyme forms contain a substoichiometric amount of inhibitory deoxyribonucleotide triphosphates (∼0.8 mol/mol of hTK2 subunit, where dTTP > dCTP > dATP), which affected the enzyme kinetic studies. Thus, the time course for the formation of dTMP or dCMP, with dThd or dCyd as the substrate, revealed a pronounced lag phase when the reaction was started by the simultaneous addition of substrate and phosphate donor (MgATP). Preincubation with substrate (dThd or dCyd), however, resulted in a dissociation of the inhibitory triphosphates (Figure 5), and a linear time course was obtained. Therefore, a preincubation with dThd or dCyd was routinely performed in the kinetic studies. No significant differences were observed between the tetrameric and dimeric forms of the enzyme, which were found to preserve their oligomeric state at concentrations as low as 0.05 mg/mL (see Results). Thus, the functional unit of hTK2 appears to be a dimer and the tetramer assembled as a dimer of dimers. A striking feature of both oligomers is that the substrates (dThd and dCyd) appear to bind to the enzyme with different affinities at low and high substrate concentrations, as seen from the Hill plots (Figure 6 and Table 1). Accordingly, the binding of dCyd revealed an apparent negative kinetic cooperativity ($h \approx 0.7$) above 4 μM and no significant cooperativity ($h \approx 0.9$) below this concentration, whereas the binding of dThd revealed an apparent negative kinetic cooperativity at substrate concentrations above ($h \approx 0.7$) and below ($h \approx$

0.5) 4 μM. Interestingly, as in the steady-state kinetic analysis, the tryptophan fluorescence measurements revealed a biphasic concentration dependence for the quenching effect of added dThd, with a negative cooperativity at low substrate concentrations (<5 μM; $h = 0.53-0.56$). The $[S]_{0.5}$ values obtained from the binding isotherms of dThd (at concentrations of >5 μM) and MgATP were ~10-fold higher than the measured K_m values in the steady-state kinetic analysis involving a 5 min preincubation period with dThd. Negative cooperativity has been observed previously for dThd with recombinant hTK2, but no mixed cooperative behavior was reported (*6*, *29*). However, these kinetic studies were performed without preincubation with substrate in the assay and at a higher temperature (37 °C vs the temperature of 25 °C used in this study). The relatively long lag phase seen in the time course experiments when no preincubation was performed (Figure 5) was to be expected for a tight binding of the deoxyribonucleoside triphosphates, and their rate of release may depend on both the substrate concentration and the temperature in the assay. Further characterization of the endogenously inhibited and the inhibitor-free enzymes will be required to gain further insight into the unusual kinetic behavior of our recombinant enzyme.

CONCLUDING REMARKS

In resting cells, the biosynthesis of dNTPs is still crucial due to the constant need of nucleotides for mtDNA replication, which occurs throughout the cell cycle, as well as for nuclear and mitochondrial DNA repair. Since *de novo* synthesis is absent in nondividing cells, the nucleotide pools have to be maintained solely via the salvage pathway of deoxyribonucleosides. In this scenario, TK2 is the only dThd phosphorylating enzyme present in cells due to the strictly S phase-correlated expression of TK1 (reviewed in ref *42*), and thus, the existence of a cytosolic form of hTK2 may be centrally important for the maintenance of a basal cytosolic pool of dTTP, considering the physical separation between the mitochondrial and cytosolic dNTP pools (*65*).

The dNTP pools in resting cells are regulated by at least two different mechanisms: (i) by the opposing irreversible reactions catalyzed by deoxyribonucleoside kinases and deoxyribonucleotidases (*66*−*68*) and (ii) by feedback inhibition of the kinases by dNTPs, the end products of the salvage pathway. The last mechanism appears to play an essential role in the regulation of deoxyribonucleoside kinases considering the nearly stoichiometric amount of inhibitors recovered bound to a purified recombinant hTK2. As far as we know, this is the first demonstration of a marked and specific inhibition of a mammalian 2′-deoxynucleoside kinase, retained from its recombinant expression in *E. coli*, and it seems quite likely that previous characterizations of at least hTK2 were performed on a partially inhibited enzyme. In such a case, it is reasonable to expect K_i values for the different inhibitors of hTK2 that are lower than the ones reported so far (*6*, *38*−*40*, *69*). In fact, conflicting results have been reported related to the affinity of the enzyme for dTTP. When purified native hTK2 was photoaffinity labeled with dTTP, the concentration giving 50% of the maximal incorporation was 20 nM (*3*), which is in contrast to the 100−350-fold higher K_i values (2−7 μM) reported for both the recombinant (*6*) and native (*39*) enzymes. Moreover, a fully active, noninhibited hTK2 may exhibit enhanced efficiency in the phosphorylation of its substrates and several nucleoside analogues or even be able to use compounds previously reported not to be substrates for the enzyme, with obvious consequences in terms of biological side effects observed for the different analogues. The widely used anti-HIV nucleoside analogue 3′-azidothymidine (AZT), known to cause severe side effects due to mitochondrial DNA damage (*70*−*72*), was shown to be poorly phosphorylated by native, purified hTK2 (*39*, *73*) but not at all by the recombinant protein (*8*). Thus, in future studies on this group of enzymes, it will be important to be aware of the possible presence of endogenous inhibitors, in both recombinant and native enzymes.

ACKNOWLEDGMENT

We thank Cand. Scient. Knut Teigen for his expert technical advice and assistance in the molecular docking experiments.

REFERENCES

1. Arnér, E. S., and Eriksson, S. (1995) Mammalian deoxyribonucleoside kinases, *Pharmacol. Ther. 67*, 155−186.
2. Hatzis, P., Al-Madhoon, A. S., Jüllig, M., Petrakis, T. G., Eriksson, S., and Talianidis, I. (1998) The intracellular localization of deoxycytidine kinase, *J. Biol. Chem. 273*, 30239−30243.
3. Jansson, O., Bohman, C., Munch-Petersen, B., and Eriksson, S. (1992) Mammalian thymidine kinase 2. Direct photoaffinity labeling with [^{32}P]dTTP of the enzyme from spleen, liver, heart and brain, *Eur. J. Biochem. 206*, 485−490.
4. Jüllig, M., and Eriksson, S. (2000) Mitochondrial and submitochondrial localization of human deoxyguanosine kinase, *Eur. J. Biochem. 267*, 5466−5472.
5. Kit, S., and Leung, W. C. (1974) Submitochondrial localization and characteristics of thymidine kinase molecular forms in parental and kinase-deficient HeLa cells, *Biochem. Genet. 11*, 231−247.
6. Wang, L., Saada, A., and Eriksson, S. (2003) Kinetic properties of mutant human thymidine kinase 2 suggest a mechanism for mitochondrial DNA depletion myopathy, *J. Biol. Chem. 278*, 6963−6968.
7. Söderlund, J. C., and Arnér, E. S. (1994) Mitochondrial versus cytosolic activities of deoxyribonucleoside salvage enzymes, *Adv. Exp. Med. Biol. 370*, 201−204.
8. Johansson, M., and Karlsson, A. (1997) Cloning of the cDNA and chromosome localization of the gene for human thymidine kinase 2, *J. Biol. Chem. 272*, 8454−8458.
9. Johansson, M., Brismar, S., and Karlsson, A. (1997) Human deoxycytidine kinase is located in the cell nucleus, *Proc. Natl. Acad. Sci. U.S.A. 94*, 11941−11945.
10. Elholm, M., Hollås, H., Issalene, C., Barroso, J. F., Berge, R. K., and Flatmark, T. (2001) Transient up-regulation of liver mitochondrial thymidine kinase activity in proliferating mitochondria, *IUBMB Life 51*, 99−104.
11. Mandel, H., Szargel, R., Labay, V., Elpeleg, O., Saada, A., Shalata, A., Anbinder, Y., Berkowitz, D., Hartman, C., Barak, M., Eriksson, S., and Cohen, N. (2001) The deoxyguanosine kinase gene is mutated in individuals with depleted hepatocerebral mitochondrial DNA, *Nat. Genet. 29*, 337−341.
12. Saada, A., Shaag, A., Mandel, H., Nevo, Y., Eriksson, S., and Elpeleg, O. (2001) Mutant mitochondrial thymidine kinase in mitochondrial DNA depletion myopathy, *Nat. Genet. 29*, 342−344.
13. Taanman, J. W., Kateeb, I., Muntau, A. C., Jaksch, M., Cohen, N., and Mandel, H. (2002) A novel mutation in the deoxyguanosine kinase gene causing depletion of mitochondrial DNA, *Ann. Neurol. 52*, 237−239.
14. Ikeda, S., Chakravarty, R., and Ives, D. H. (1986) Multisubstrate analogs for deoxynucleoside kinases. Triphosphate end products and synthetic bisubstrate analogs exhibit identical modes of binding and are useful probes for distinguishing kinetic mechanisms, *J. Biol. Chem. 261*, 15836−15843.

15. Kim, M. Y., and Ives, D. H. (1989) Human deoxycytidine kinase: kinetic mechanism and end product regulation, *Biochemistry 28*, 9043−9047.
16. Mikkelsen, N. E., Johansson, K., Karlsson, A., Knecht, W., Andersen, G., Piškur, J., Munch-Petersen, B., and Eklund, H. (2003) Structural Basis for Feedback Inhibition of the Deoxyribonucleoside Salvage Pathway: Studies of the *Drosophila* Deoxyribonucleoside Kinase, *Biochemistry 42*, 5706−5712.
17. Johansson, K., Ramaswamy, S., Ljungcrantz, C., Knecht, W., Piškur, J., Munch-Petersen, B., Eriksson, S., and Eklund, H. (2001) Structural basis for substrate specificities of cellular deoxyribonucleoside kinases, *Nat. Struct. Biol. 8*, 616−620.
18. di Guan, C., Li, P., Riggs, P. D., and Inouye, H. (1988) Vectors that facilitate the expression and purification of foreign peptides in *Escherichia coli* by fusion to maltose-binding protein, *Gene 67*, 21−30.
19. Haarr, L., and Flatmark, T. (1987) Evidence that deletion of coding sequences in the 5′ end of the thymidine kinase gene of herpes simplex virus type 1 affects the stability of the gene products, *J. Gen. Virol. 68*, 2817−2829.
20. Guex, N., and Peitsch, M. C. (1997) SWISS-MODEL and the Swiss-PdbViewer: an environment for comparative protein modeling, *Electrophoresis 18*, 2714−2723.
21. Peitsch, M. C. (1995) Protein modeling by E-mail, *Bio/Technology 13*, 658−660.
22. Peitsch, M. C. (1996) ProMod and Swiss-Model: Internet-based tools for automated comparative protein modelling, *Biochem. Soc. Trans. 24*, 274−279.
23. Kuntz, I. D. (1992) Structure-based strategies for drug design and discovery, *Science 257*, 1078−1082.
24. Kuntz, I. D., Meng, E. C., and Shoichet, B. K. (1994) Structure-based molecular design, *Acc. Chem. Res. 27*, 117−123.
25. Ferrin, T. E., Huang, C. C., Jarvis, L. E., and Langridge, R. (1988) The MIDAS Display System, *J. Mol. Graphics 6*, 13−27.
26. Kuntz, I. D., Blaney, J. M., Oatley, S. J., Langridge, R., and Ferrin, T. E. (1982) A geometric approach to macromolecule-ligand interactions, *J. Mol. Biol. 161*, 269−288.
27. Meng, E. C., Shoichet, B. K., and Kuntz, I. D. (1992) Automated docking with grid-based energy evaluation, *J. Comput. Chem. 13*, 505−524.
28. Shoichet, B. K., Bodian, D. L., and Kuntz, I. D. (1992) Molecular docking using shape descriptors, *J. Comput. Chem. 13*, 380−397.
29. Wang, L., Munch-Petersen, B., Herrström Sjöberg, A., Hellman, U., Bergman, T., Jörnvall, H., and Eriksson, S. (1999) Human thymidine kinase 2: molecular cloning and characterisation of the enzyme activity with antiviral and cytostatic nucleoside substrates, *FEBS Lett. 443*, 170−174.
30. Lander, E. S., Linton, L. M., Birren, B., Nusbaum, C., Zody, M. C., Baldwin, J., Devon, K., Dewar, K., Doyle, M., FitzHugh, W., Funke, R., Gage, D., Harris, K., Heaford, A., Howland, J., Kann, L., Lehoczky, J., LeVine, R., McEwan, P., McKernan, K., Meldrim, J., Mesirov, J. P., Miranda, C., Morris, W., Naylor, J., Raymond, C., Rosetti, M., Santos, R., Sheridan, A., Sougnez, C., Stange-Thomann, N., Stojanovic, N., Subramanian, A., Wyman, D., Rogers, J., Sulston, J., Ainscough, R., Beck, S., Bentley, D., Burton, J., Clee, C., Carter, N., Coulson, A., Deadman, R., Deloukas, P., Dunham, A., Dunham, I., Durbin, R., French, L., Grafham, D., Gregory, S., Hubbard, T., Humphray, S., Hunt, A., Jones, M., Lloyd, C., McMurray, A., Matthews, L., Mercer, S., Milne, S., Mullikin, J. C., Mungall, A., Plumb, R., Ross, M., Shownkeen, R., Sims, S., Waterston, R. H., Wilson, R. K., Hillier, L. W., McPherson, J. D., Marra, M. A., Mardis, E. R., Fulton, L. A., Chinwalla, A. T., Pepin, K. H., Gish, W. R., Chissoe, S. L., Wendl, M. C., Delehaunty, K. D., Miner, T. L., Delehaunty, A., Kramer, J. B., Cook, L. L., Fulton, R. S., Johnson, D. L., Minx, P. J., Clifton, S. W., Hawkins, T., Branscomb, E., Predki, P., Richardson, P., Wenning, S., Slezak, T., Doggett, N., Cheng, J. F., Olsen, A., Lucas, S., Elkin, C., Uberbacher, E., Frazier, M., *et al*. (2001) Initial sequencing and analysis of the human genome, *Nature 409*, 860−921.
31. Knecht, W., Petersen, G. E., Munch-Petersen, B., and Piškur, J. (2002) Deoxyribonucleoside kinases belonging to the thymidine kinase 2 (TK2)-like group vary significantly in substrate specificity, kinetics and feed-back regulation, *J. Mol. Biol. 315*, 529−540.
32. Bordo, D., and Argos, P. (1991) Suggestions for "safe" residue substitutions in site-directed mutagenesis, *J. Mol. Biol. 217*, 721−729.
33. Steczko, J., Donoho, G. A., Dixon, J. E., Sugimoto, T., and Axelrod, B. (1991) Effect of ethanol and low-temperature culture on expression of soybean lipoxygenase L-1 in *Escherichia coli*, *Protein Expression Purif. 2*, 221−227.
34. Thomas, J. G., and Baneyx, F. (1996) Protein misfolding and inclusion body formation in recombinant *Escherichia coli* cells overexpressing heat-shock proteins, *J. Biol. Chem. 271*, 11141−11147.
35. Thomas, J. G., and Baneyx, F. (1997) Divergent effects of chaperone overexpression and ethanol supplementation on inclusion body formation in recombinant *Escherichia coli*, *Protein Expression Purif. 11*, 289−296.
36. Wang, L., and Eriksson, S. (2000) Cloning and characterization of full-length mouse thymidine kinase 2: the N-terminal sequence directs import of the precursor protein into mitochondria, *Biochem. J. 351*, 469−476.
37. Munch-Petersen, B., Piškur, J., and Søndergaard, L. (1998) Four deoxynucleoside kinase activities from *Drosophila melanogaster* are contained within a single monomeric enzyme, a new multifunctional deoxynucleoside kinase, *J. Biol. Chem. 273*, 3926−3931.
38. Lee, L. S., and Cheng, Y. (1976) Human deoxythymidine kinase II: substrate specificity and kinetic behavior of the cytoplasmic and mitochondrial isozymes derived from blast cells of acute myelocytic leukemia, *Biochemistry 15*, 3686−3690.
39. Munch-Petersen, B., Cloos, L., Tyrsted, G., and Eriksson, S. (1991) Diverging substrate specificity of pure human thymidine kinases 1 and 2 against antiviral dideoxynucleosides, *J. Biol. Chem. 266*, 9032−9038.
40. Ellims, P. H., and Van der Weyden, M. B. (1981) Kinetic mechanism and inhibition of human liver thymidine kinase, *Biochim. Biophys. Acta 660*, 238−242.
41. Johansson, M., van Rompay, A. R., Degrève, B., Balzarini, J., and Karlsson, A. (1999) Cloning and characterization of the multisubstrate deoxyribonucleoside kinase of *Drosophila melanogaster*, *J. Biol. Chem. 274*, 23814−23819.
42. Eriksson, S., Munch-Petersen, B., Johansson, K., and Eklund, H. (2002) Structure and function of cellular deoxyribonucleoside kinases, *Cell. Mol. Life Sci. 59*, 1327−1346.
43. Wild, K., Bohner, T., Folkers, G., and Schulz, G. E. (1997) The structures of thymidine kinase from *Herpes simplex* virus type 1 in complex with substrates and a substrate analogue, *Protein Sci. 6*, 2097−2106.
44. Wettin, K., Johansson, M., Zheng, X., Zhu, C., and Karlsson, A. (1999) Cloning of mouse mitochondrial thymidine kinase 2 cDNA, *FEBS Lett. 460*, 103−106.
45. Petrakis, T. G., Ktistaki, E., Wang, L., Eriksson, S., and Talianidis, I. (1999) Cloning and characterization of mouse deoxyguanosine kinase. Evidence for a cytoplasmic isoform, *J. Biol. Chem. 274*, 24726−24730.
46. Nilsen, H., Otterlei, M., Haug, T., Solum, K., Nagelhus, T. A., Skorpen, F., and Krokan, H. E. (1997) Nuclear and mitochondrial uracil-DNA glycosylases are generated by alternative splicing and transcription from different positions in the *UNG* gene, *Nucleic Acids Res. 25*, 750−755.
47. Ladner, R. D., and Caradonna, S. J. (1997) The human dUTPase gene encodes both nuclear and mitochondrial isoforms. Differential expression of the isoforms and characterization of a cDNA encoding the mitochondrial species, *J. Biol. Chem. 272*, 19072−19080.
48. Tolkunova, E., Park, H., Xia, J., King, M. P., and Davidson, E. (2000) The human lysyl-tRNA synthetase gene encodes both the cytoplasmic and mitochondrial enzymes by means of an unusual alternative splicing of the primary transcript, *J. Biol. Chem. 275*, 35063−35069.
49. Wang, L. (1997) Mitochondrial deoxyribonucleoside salvage enzymes: cloning and characterization of deoxyguanosine kinase and thymidine kinase, *Acta Univ. Agric. Sueciae-Veterinaria 7*, ISSN 1401-6257, ISBN 1491-1576-5235-X.
50. Sigler, P. B., Xu, Z., Rye, H. S., Burston, S. G., Fenton, W. A., and Horwich, A. L. (1998) Structure and function in GroEL-mediated protein folding, *Annu. Rev. Biochem. 67*, 581−608.
51. Richardson, A., Landry, S. J., and Georgopoulos, C. (1998) The ins and outs of a molecular chaperone machine, *Trends Biochem. Sci. 23*, 138−143.
52. Gottesman, M. E., and Hendrickson, W. A. (2000) Protein folding and unfolding by *Escherichia coli* chaperones and chaperonins, *Curr. Opin. Microbiol. 3*, 197−202.

53. Neidhardt, F. C., and VanBogelen, R. A. (1987) The heat shock response, in *Escherichia coli and Salmonella typhimurium*: Cellular and Molecular Biology (Neidhardt, F. C., Ingraham, J. L., Low, K. B., Magasanik, B., Schaecter, M., and Umbarger, H. E., Eds.) pp 1334−1345, American Society for Microbiology, Washington, DC.
54. VanBogelen, R. A., Kelley, P. M., and Neidhardt, F. C. (1987) Differential induction of heat shock, SOS, and oxidation stress regulons and accumulation of nucleotides in *Escherichia coli*, *J. Bacteriol. 169*, 26−32.
55. Yura, T., Nagai, H., and Mori, H. (1993) Regulation of the heat-shock response in bacteria, *Annu. Rev. Microbiol. 47*, 321−350.
56. Gragerov, A., Nudler, E., Komissarova, N., Gaitanaris, G. A., Gottesman, M. E., and Nikiforov, V. (1992) Cooperation of GroEL/GroES and DnaK/DnaJ heat shock proteins in preventing protein misfolding in *Escherichia coli*, *Proc. Natl. Acad. Sci. U.S.A. 89*, 10341−10344.
57. Langer, T., Lu, C., Echols, H., Flanagan, J., Hayer, M. K., and Hartl, F. U. (1992) Successive action of DnaK, DnaJ and GroEL along the pathway of chaperone-mediated protein folding, *Nature 356*, 683−689.
58. Goloubinoff, P., Mogk, A., Zvi, A. P., Tomoyasu, T., and Bukau, B. (1999) Sequential mechanism of solubilization and refolding of stable protein aggregates by a bichaperone network, *Proc. Natl. Acad. Sci. U.S.A. 96*, 13732−13737.
59. Hartl, F. U. (1991) Heat shock proteins in protein folding and membrane translocation, *Semin. Immunol. 3*, 5−16.
60. Schwarz, E., and Neupert, W. (1994) Mitochondrial protein import: mechanisms, components and energetics, *Biochim. Biophys. Acta 1187*, 270−274.
61. Stuart, R. A., Cyr, D. M., Craig, E. A., and Neupert, W. (1994) Mitochondrial molecular chaperones: their role in protein translocation, *Trends Biochem. Sci. 19*, 87−92.
62. Crookes, W. J., and Olsen, L. J. (1998) The effects of chaperones and the influence of protein assembly on peroxisomal protein import, *J. Biol. Chem. 273*, 17236−17242.
63. Brown, D. G., Visse, R., Sandhu, G., Davies, A., Rizkallah, P. J., Melitz, C., Summers, W. C., and Sanderson, M. R. (1995) Crystal structures of the thymidine kinase from herpes simplex virus type-I in complex with deoxythymidine and ganciclovir, *Nat. Struct. Biol. 2*, 876−881.
64. Munch-Petersen, B., Knecht, W., Lenz, C., Søndergaard, L., and Piškur, J. (2000) Functional expression of a multisubstrate deoxyribonucleoside kinase from *Drosophila melanogaster* and its C-terminal deletion mutants, *J. Biol. Chem. 275*, 6673−6679.
65. Traut, T. W. (1994) Physiological concentrations of purines and pyrimidines, *Mol. Cell. Biochem. 140*, 1−22.
66. Reichard, P. (1988) Interactions between deoxyribonucleotide and DNA synthesis, *Annu. Rev. Biochem. 57*, 349−374.
67. Rampazzo, C., Gallinaro, L., Milanesi, E., Frigimelica, E., Reichard, P., and Bianchi, V. (2000) A deoxyribonucleotidase in mitochondria: involvement in regulation of dNTP pools and possible link to genetic disease, *Proc. Natl. Acad. Sci. U.S.A. 97*, 8239−8244.
68. Gazziola, C., Ferraro, P., Moras, M., Reichard, P., and Bianchi, V. (2001) Cytosolic high K_m 5′-nucleotidase and 5′(3′)-deoxyribonucleotidase in substrate cycles involved in nucleotide metabolism, *J. Biol. Chem. 276*, 6185−6190.
69. Munch-Petersen, B. (1984) Differences in the kinetic properties of thymidine kinase isoenzymes in unstimulated and phytohemagglutinin-stimulated human lymphocytes, *Mol. Cell. Biochem. 64*, 173−185.
70. Arnaudo, E., Dalakas, M., Shanske, S., Moraes, C. T., DiMauro, S., and Schon, E. A. (1991) Depletion of muscle mitochondrial DNA in AIDS patients with zidovudine-induced myopathy, *Lancet 337*, 508−510.
71. Casademont, J., Barrientos, A., Grau, J. M., Pedrol, E., Estivill, X., Urbano-Márquez, A., and Nunes, V. (1996) The effect of zidovudine on skeletal muscle mtDNA in HIV-1 infected patients with mild or no muscle dysfunction, *Brain 119*, 1357−1364.
72. Lewis, W., Papoian, T., Gonzalez, B., Louie, H., Kelly, D. P., Payne, R. M., and Grody, W. W. (1991) Mitochondrial ultrastructural and molecular changes induced by zidovudine in rat hearts, *Lab. Invest. 65*, 228−236.
73. Eriksson, S., Kierdaszuk, B., Munch-Petersen, B., Öberg, B., and Johansson, N. G. (1991) Comparison of the substrate specificities of human thymidine kinase 1 and 2 and deoxycytidine kinase toward antiviral and cytostatic nucleoside analogs, *Biochem. Biophys. Res. Commun. 176*, 586−592.

BI035230F